Solid Freeform Fabrication 2024: Proceedings of the 35th Annual International Solid Freeform Fabrication Symposium – An Additive Manufacturing Conference
Reviewed Paper

ON THE NATURE OF RECOATER DAMAGE POWDER SPREADING MECHANICS

Caroline E. Massey*, Christopher J. Saldaña*

*George W. Woodruff School of Mechanical Engineering, Georgia Institute of Technology, 801 Ferst Drive NW Atlanta, GA 30332

Keywords: Laser Powder Bed Fusion, In-Situ Monitoring, Powder Spreading, Recoater Damage

Abstract

Laser powder bed fusion (PBF-LB) additive manufacturing gained popularity for the creation of high mix, low volume parts for defense and commercial applications. Parts made via PBF-LB can be difficult to qualify due to their variation in performance, even within the same build. During the build process, regions of the PBF-LB recoater blade could be subject to damage by spatter or superelevation in the powder bed. As a result, the worn recoater can potentially cause spreading defects in the localized topography profile, which could in turn cause porosity or form deviations. These process concerns are not well understood for their criticality and subsequent impact on part quality. This study will investigate the mechanics of recoater damage through two experimental builds. Post-mortem inspection of the failure region will be conducted with laser line profilometry and will help propose a better understanding of the criticality of extreme recoater damage.

Introduction

Laser powder bed fusion presents an opportunity for parts to be made on demand, often a significant time savings from the planning and logistics required to operate the conventional factory casting process line. The qualification and certification of additively manufactured parts can be difficult due to their stochastic behavior, especially in fatigue [1]. These parts can be exposed to local changes in process conditions which can potentially affect part quality or even lead to build failure. One such local processing condition is the exposure to recoater damage on the blade. Recoater damage often occurs due to superelevations in the build process or spatter colliding with the recoater and causing wear to occur [2], [3].

The geometry and material selection of the recoater is often tailored to the machine constraints and parts to be manufactured. Many works have studied the spreading process through discrete element method (DEM) simulations to understand how process parameters impact the quality of the powder bed [4], [5], [6]. Such tests have even been done with different types of recoaters to study the effect of different geometric profiles and materials with both DEM and in-situ methods [7], [8], [9]. Hard recoater blades are often selected because their stiffness allows them to remove spatter and superelevation that is above the layer height at the deposited layer, yielding to more flatness in the powder bed, at the expense of being prone to collisions and jamming. To date, prior studies have not investigated the impact of intentional recoater damage induced within the hard recoater blade.

Mechanical properties and the porosity profile of the part can be significantly impacted by recoater wear. Horizontal streaking often occurs in regions of the powder bed that are subjected to a worn recoater [10], [11]. Excess porosity has been shown to have an impact on the mechanical performance of tensile specimens [12]. In a study using intentionally damaged electron beam powder bed fusion (PBF-EB) brush recoaters, the authors found that the porosity in regions impacted by local recoater damage was much higher than non-affected regions [13]. The study found that pores in worn recoater regions resembled that of lack of fusion porosity. Lack of fusion

pores are especially detrimental to mechanical performance as they are larger than gas porosity, are highly irregular, and can serve as initiation sites for failure [14].

Previous researchers have understood the detectability of recoater damage using machine learning and computer vision techniques [11], [15], [16]. Others have attempted to simulate the onset of recoater damage using parts that will cause intentional superelevation interactions with the recoater [17]. These prior works have not addressed the criticality of the size of the wear profile on the hard recoater blade. These works have also not studied the mechanics of how recoater damage can cause build failure. The present work will address the mechanics of recoater damage with extreme wear conditions through two investigational builds. The surface topography deviations of the as-printed parts will be addressed as well as the deviations in a pre-spread sample first layer. These form deviations will be evaluated with laser line profilometry.

Materials and Methods

This work used two builds to study the mechanics of spreading with a worn recoater. The first experiment used a build plate layout consisting of a series of bar coupons. The second experiment build plate had a series of bar coupons and parts based on the geometry of ASTM E8 specimens [18]. The build plate design for both experiments is shown in Figure 1. The first experiment used Kennametal Stainless Steel 316L powders that had been sieved six times with a D10 of 14.5 micron, D50 of 20.7 micron, and D90 of 31.6 micron. The second experiment used one-time sieved Carpenter Additive 316L powders with a D10 of 21.3 micron, D50 of 29.5 micron, and D90 of 43.4 micron. Both powder size distributions were measured on a Malvern Mastersizer 3000. The number density powder size distribution for both experiments is shown in Figure 2. All prints were conducted on an EOS M280 using 928.1 mm/s speed, 214.2 W power, and a hatch spacing of 0.10 mm with rotated and alternating hatch spacing. The dosing factor of the second experiment was slightly larger to account for the larger D50 values.

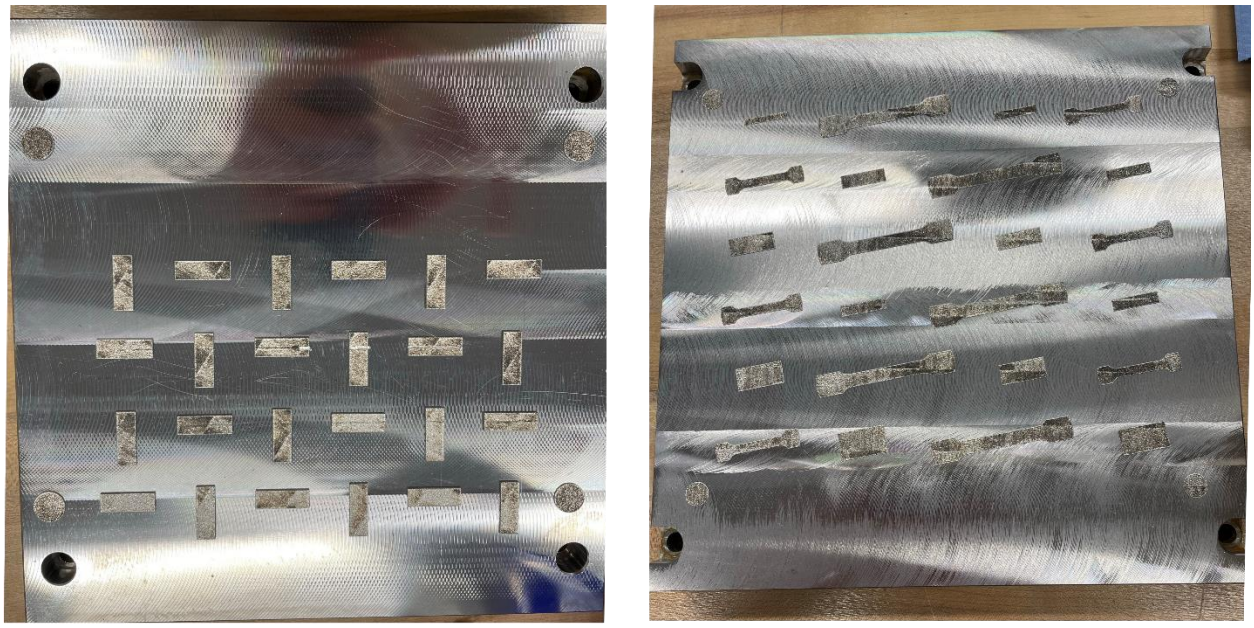

a) b)

Figure 1: a) Set-up of the build plate in experiment 1 b) build plate design in experiment 2

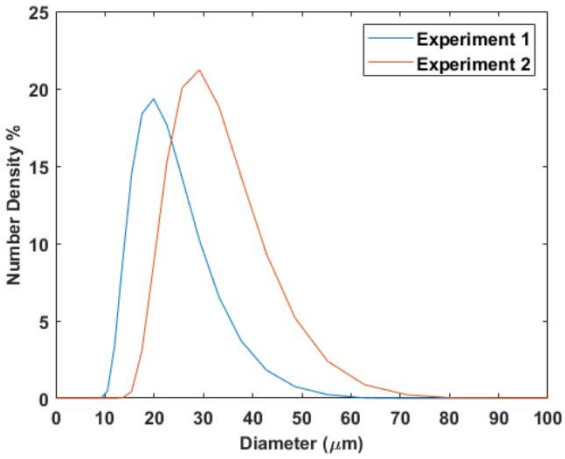

Figure 2: PSD Compositions of the 316L powders used in experiments 1 and 2

All recoaters used were purchased directly from the manufacturer and were made of high-speed steel. The recoater used in experiment 1 had notch damage that was created via an electric discharge machine (EDM), the size of the damage based on the size of notch damage in previously worn recoaters and EDM limits. The recoater used in the second experiment had notch wear that was also created via EDM. The smallest notch in both experiments was the smallest notch feasible with the EDM setup. Figure 3 shows the positioning of the recoater damage and the size of the recoater damage is shown in Table 1. These images and measurements were captured on a Keyence VR6000 Series optical profilometer in low magnification mode with a magnification of 12x. Additional images of the recoater blade after failure were captured on a Dyno-lite digital microscope.

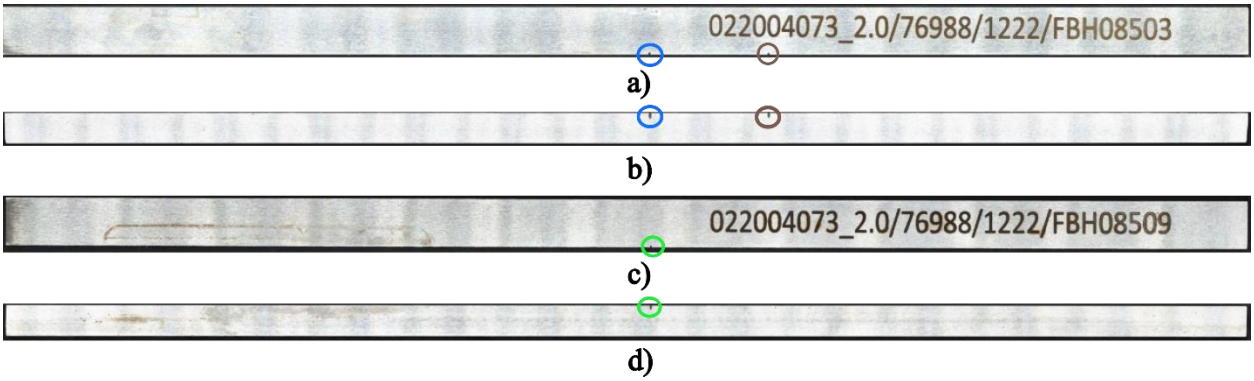

Figure 3: Recoater bar used in experiment 1 a) front view b) side view. Recoater bar used in experiment 2 c) front view d) side view.

Table 1: Wear profile in experiments 1 and 2

Experiment Number	Labeled Color	Length (mm)	Width (mm)	Depth (mm)
Experiment 1	Brown	0.394	0.439	1.063
Experiment 1	Blue	0.461	0.518	1.285
Experiment 2	Green	0.377	0.459	0.867

The as printed parts were scanned with a Keyence LJ-X8080 laser line profiler using 8000 lines and a 12.5 micron x, y, and z resolution. The laser line profiler was affixed to the recoater arm assembly by a custom mount and is shown in Figure 4 below. The laser line profiler was able to capture a sample first layer profile of the spread powder in experiment 2. The output profile was analyzed using modified MATLAB code that had been developed by previous researchers [8]. A Dyno-lite digital microscope was used to capture images of the part surfaces.

Figure 4: Keyence LJ-X8080 setup in EOS M280 capturing the part surfaces of experiment 1

Results and Discussion

In the first experiment, build failure occurred in the region of the largest recoater damage, as shown in Figure 5 below. Hard recoater blades by their nature will work to shear any part deviations above the layer thickness. In the worn region where significant notch damage is present, any deviations will be allowed to pass until they form above the tallest section of the notch, or spatter or other bed defects get caught in the notch opening. Based on inspection of the post-mortem images, it appears that once spatter or superelevated debris got trapped in the notch, it at some point interacted with the superelevated regions and appeared to roll and pick up molten superelevated material or spatter, forming a bead. As the bead picks up material, it will leave the previous region with a dimple formed from removed material. The bead will become so large that it will collide with the recoater bar and cause failure.

Figure 5: Location of build failure region in experiment 1

In the case of experiment 1, approximately 0.80 mm of the build was successfully lased prior to failure. The laser line profilometry scan of the parts in the band of highest recoater damage is shown in Figure 6. The part surfaces captured with a digital microscope are shown in Figure 7. In the region subject to recoater damage and to the right of the part at failure (part C4), the formation of the rolled ball bead caused a local topographical loss of 0.0705 mm relative to the flat part of the fused surface. The difference is about 1.5 times the layer height so there is a potential for porosity to form in this region as result of the difference in surface topography. The rolled bead formed at the failure location caused a local topographical difference of 0.6534 mm above the fused surface, which is larger than the length of the recoater notch that it would be able to pass through (0.461 mm). To the left of the failure part section, the recoater damage caused about 0.1741 mm difference in height, which is about four times the layer height, but roughly a quarter of the length of the notch (0.461 mm). Part C6, which is to the right of the failure region has a form deviation of around .0992 mm, which is less than the region ahead of the damaged section. This means that perhaps the spatter that was stuck in the recoater notch could have sheared parts of the profile or there could also be deviations in the topography profile due to variability between parts.

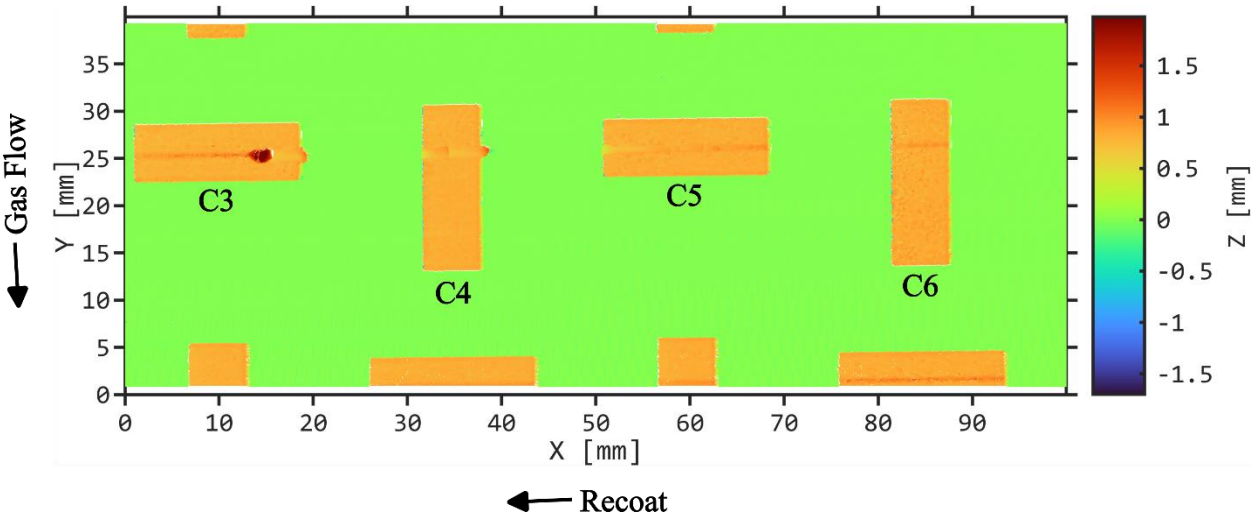

Figure 6: Topography profile of parts for experiment 1 in the region of highest recoater damage

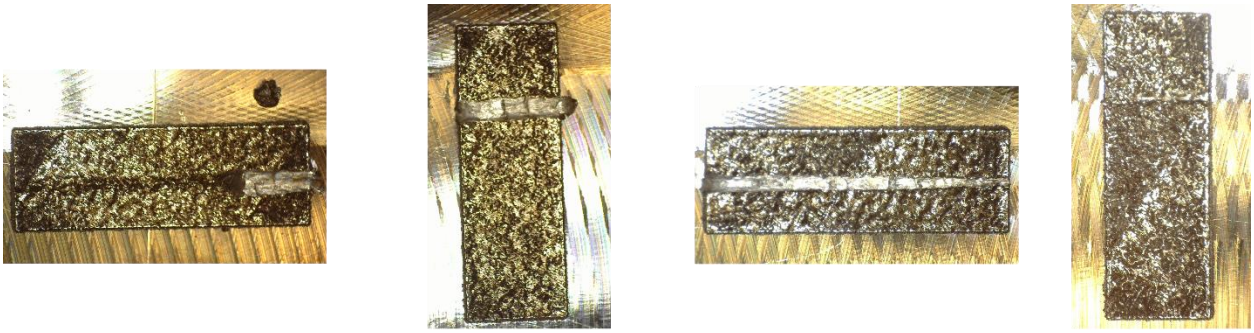

Figure 7: Parts along the larger recoater damaged section, locations corresponding with Figure 6

In the area subject to the smaller notch, the surface topology results are shown in Figure 8. In the inspection of the recoater after failure, there was a bead stuck in the recoater notch section, which is shown in Figure 9. This was likely spatter or superelevation that got caught in this section of the damaged recoater. The topography deviation in the recoater damaged section averaged over four parts in the region was 0.1388 mm, which is a bit smaller than the portion of the failure part ahead of the failure region. This deviation is much less than the length of the notch (0.394 mm). The topography deviation in the lased portion of the recoater damaged region is likely most dependent on the dosing, layer thickness, and charge amount, since the size of the notch is potentially greater than the largest forward moving front of the powder spreading profile.

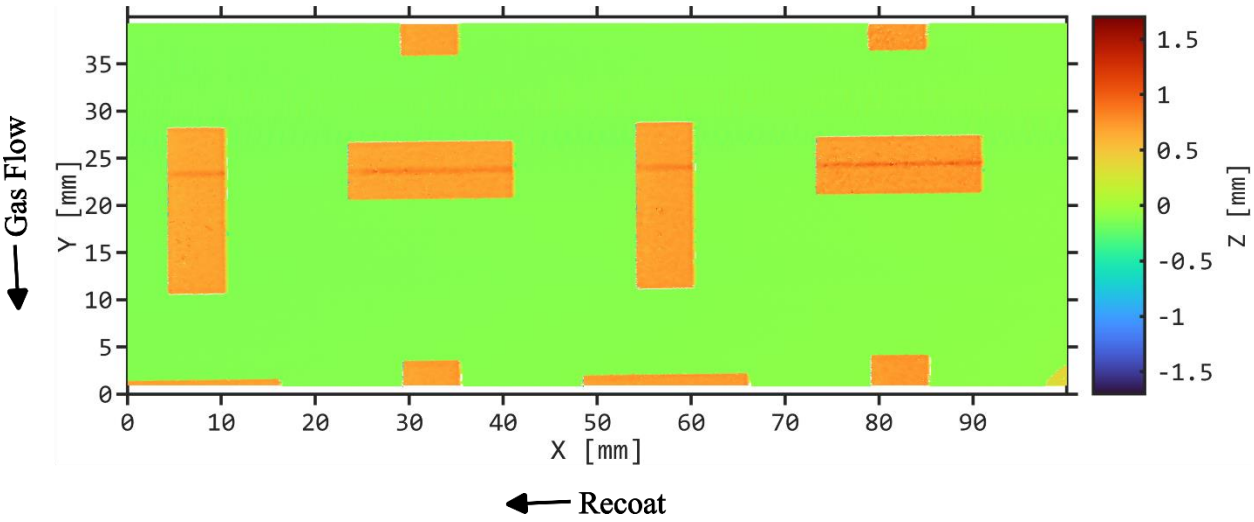

Figure 8: Topography profile in the smaller recoater damaged section of experiment 1

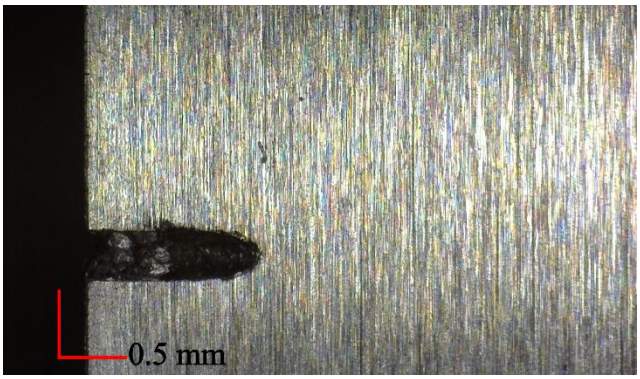

Figure 9: Bead caught in damaged recoater in small notch section of experiment 1

For experiment 2, a sample scan of the bed topography of the first layer was taken prior to starting the lasing process. The results of the powder bed in a sample 100 mm wide by 40 mm long section of the powder bed in the section subject to recoater damage is shown in Figure 10 below. Looking at the average height profile of the powder bed across the middle 60 mm of the spread direction is shown in Figure 11 below. The results indicate that the largest average deviation from the form-leveled baseline is .0328 mm which is less than one layer thickness of deviation.

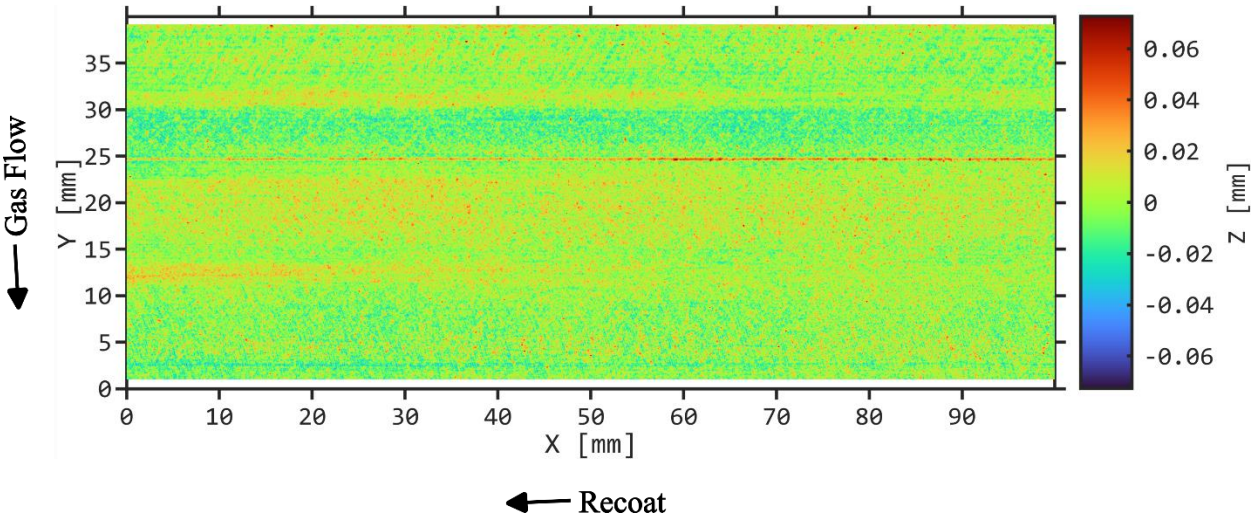

Figure 10: Sample first layer profile in recoater damaged section in experiment 2

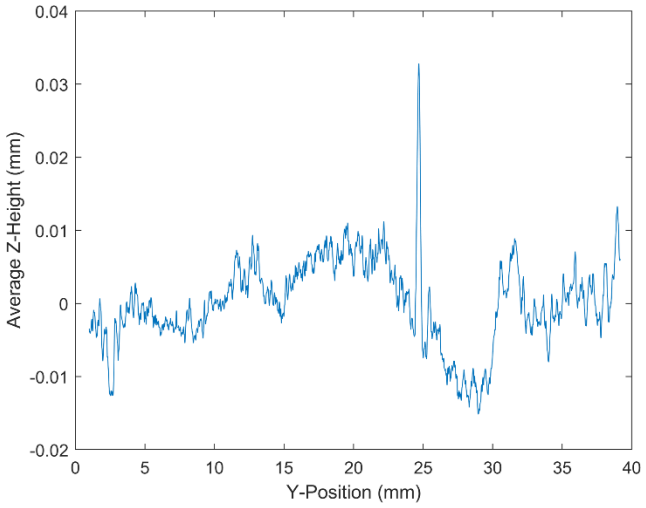

Figure 11: Average line profile in Z- direction captured at the middle 60 mm along the spread direction

The build in experiment 2 failed around 0.17 mm of build height which is earlier in the build process than experiment 1. This could be due to the different build plate configuration and larger powder size. The location of build failure is shown in Figure 12 below. The build failed in the recoater damaged region. The surface topography profile of experiment 2, subject to the smallest size of recoater damage amongst the conditions tested is shown in Figure 13 below. Much like the previous experiment, the failure region also showed the rolled ball formation at the failure site. The rolled ball formation was 0.6746 taller than the level surface. This deviation is greater than the length of the recoater notch, 0.377 mm. In this case, the parts to the right of the failure site along the damaged region, showed significant hopping behavior. In the region to the left of the failure region, the deviation in the form profile was 0.1233 mm. Since the length of damage is likely much greater than the forward moving front of the powder, the dosing amount will have more of an impact on determining the topography deviation.

Figure 12: Build failure location in experiment 2

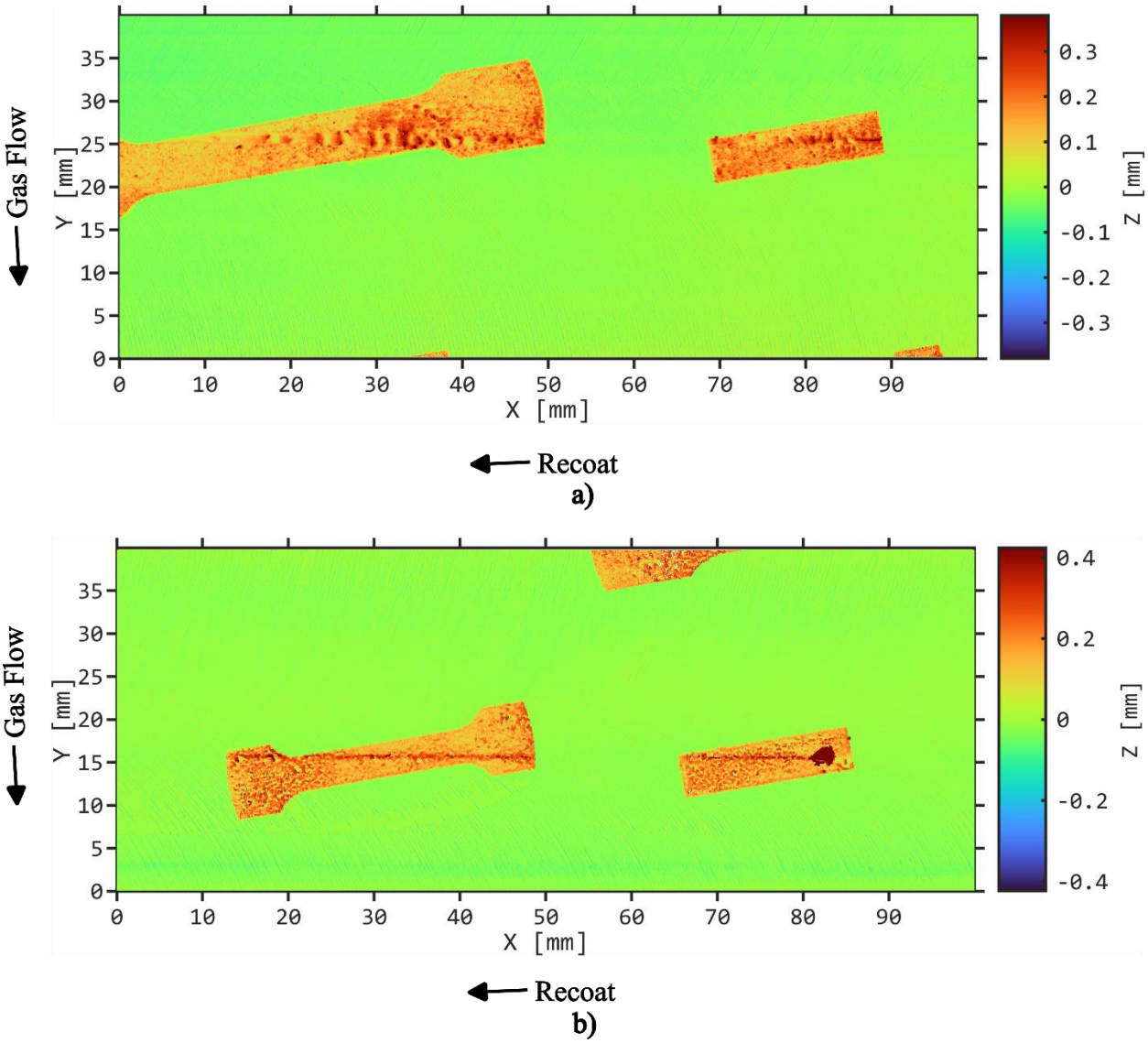

Figure 13: a) Parts to the right of the failure part along the damaged region that show hopping behavior b) Failure part and part ahead of the failure region.

This work represents an analysis of extreme recoater damage. There could exist a size of recoater damage that causes negligible difference to the spreading profile, which will be addressed in future work. This work also suggests that the notch profile provides a containment spot for spatter or removed superelevated beads to reside. These beads can fill in the gaps of the recoater damage and could initially create a more level profile in the recoater damaged section. The superelevated regions could also collide with the trapped beads and lead to shearing of the superelevated region, jamming, and build failure. The modeling of recoater damage with the EDM is imperfect as the depth must be deep due to set-up constraints. The impact of the overall shape and distribution of volume of the notch profile is of potential interest for future work.

Conclusion

The present work used two experimental builds to determine the underlying mechanics of recoater damage with extreme recoater wear. Under EDM created wear conditions, the spatter and sheared superelevation became trapped in the opening created by the worn recoater damage. These beads can shear additional superelevated material or spatter in the recoating path to create a rolled bead of material that causes the recoater arm to jam and the build to fail. The surface deviation in the parts in the regions ahead of the failure region show that the deviation is more impacted by the dosing factor and layer height, when the length of the notch is greater than the height of the spread powder forward moving front.

Acknowledgements

Thank you to Dr. Jaime Berez at UNC-Charlotte for providing the building blocks of the form leveling code used in this paper as well as helping design a new mount for the recoater arm. Thank you to the NDSEG Fellowship, DOE Grant DE-EE0008303, and LANL Award AWD-005332 for helping to fund this research. Thank you to the Montgomery Machining Mall and AMPF Staff for helping support the EDM, machining, and build set-up operations needed to complete these experiments.

References

[1] J. Berez, L. Sheridan, and C. Saldaña, "Extreme variation in fatigue: Fatigue life prediction and dependence on build volume location in laser powder bed fusion of 17-4 stainless steel," *International Journal of Fatigue*, vol. 158, p. 106737, May 2022, doi: 10.1016/j.ijfatigue.2022.106737.

[2] D. Wang *et al.*, "Mechanisms and characteristics of spatter generation in SLM processing and its effect on the properties," *Materials & Design*, vol. 117, pp. 121–130, Mar. 2017, doi: 10.1016/j.matdes.2016.12.060.

[3] R. Yavari *et al.*, "Part-scale thermal simulation of laser powder bed fusion using graph theory: Effect of thermal history on porosity, microstructure evolution, and recoater crash," *Materials & Design*, vol. 204, p. 109685, Jun. 2021, doi: 10.1016/j.matdes.2021.109685.

[4] A. Phua, P. S. Cook, C. H. J. Davies, and G. W. Delaney, "Powder spreading over realistic laser melted surfaces in metal additive manufacturing," *Additive Manufacturing Letters*, vol. 3, p. 100039, Dec. 2022, doi: 10.1016/j.addlet.2022.100039.

[5] D. Yao *et al.*, "Dynamic investigation on the powder spreading during selective laser melting additive manufacturing," *Additive Manufacturing*, vol. 37, p. 101707, Jan. 2021, doi: 10.1016/j.addma.2020.101707.

[6] Y. Lee, A. K. Gurnon, D. Bodner, and S. Simunovic, "Effect of Particle Spreading Dynamics on Powder Bed Quality in Metal Additive Manufacturing," *Integr Mater Manuf Innov*, vol. 9, no. 4, pp. 410–422, Dec. 2020, doi: 10.1007/s40192-020-00193-1.

[7] A. Phua, C. Doblin, P. Owen, C. H. J. Davies, and G. W. Delaney, "The effect of recoater geometry and speed on granular convection and size segregation in powder bed fusion," *Powder Technology*, vol. 394, pp. 632–644, Dec. 2021, doi: 10.1016/j.powtec.2021.08.058.

[8] J. Berez and C. Saldaña, “Laser Line Profile Scanning for Powder Bed Topography Measurement,” in *Solid Freeform Fabrication Symposium*, 2022, pp. 1039–1051.

[9] L. Cao, “Study on the numerical simulation of laying powder for the selective laser melting process,” *Int J Adv Manuf Technol*, vol. 105, no. 5, pp. 2253–2269, Dec. 2019, doi: 10.1007/s00170-019-04440-4.

[10] Z. Snow, L. Scime, A. Ziabari, B. Fisher, and V. Paquit, “Scalable in situ non-destructive evaluation of additively manufactured components using process monitoring, sensor fusion, and machine learning,” *Additive Manufacturing*, vol. 78, p. 103817, Sep. 2023, doi: 10.1016/j.addma.2023.103817.

[11] T. Craeghs, S. Clijsters, E. Yasa, and J.-P. Kruth, “Online Quality Control of Selective Laser Melting,” in *2011 International Solid Freeform Fabrication Symposium*, 2011.

[12] S. Cacace, L. Pagani, B. M. Colosimo, and Q. Semeraro, “The effect of energy density and porosity structure on tensile properties of 316L stainless steel produced by laser powder bed fusion,” *Prog Addit Manuf*, vol. 7, no. 5, pp. 1053–1070, Oct. 2022, doi: 10.1007/s40964-022-00281-y.

[13] M. Grasso, “In Situ Monitoring of Powder Bed Fusion Homogeneity in Electron Beam Melting,” *Materials*, vol. 14, no. 22, p. 7015, Nov. 2021, doi: 10.3390/ma14227015.

[14] F. H. Kim, S. P. Moylan, T. Q. Phan, and E. J. Garboczi, “Investigation of the Effect of Artificial Internal Defects on the Tensile Behavior of Laser Powder Bed Fusion 17–4 Stainless Steel Samples: Simultaneous Tensile Testing and X-Ray Computed Tomography,” *Exp Mech*, vol. 60, no. 7, pp. 987–1004, Sep. 2020, doi: 10.1007/s11340-020-00604-6.

[15] L. Scime and J. Beuth, “A multi-scale convolutional neural network for autonomous anomaly detection and classification in a laser powder bed fusion additive manufacturing process,” *Additive Manufacturing*, vol. 24, pp. 273–286, Dec. 2018, doi: 10.1016/j.addma.2018.09.034.

[16] L. Scime and J. Beuth, “Anomaly detection and classification in a laser powder bed additive manufacturing process using a trained computer vision algorithm,” *Additive Manufacturing*, vol. 19, pp. 114–126, Jan. 2018, doi: 10.1016/j.addma.2017.11.009.

[17] S. Brenner, M. Moser, L. Strauß, V. Nedeljkovic-Groha, and G. Löwisch, “Recoater crashes during powder bed fusion of metal with laser beam: simulative prediction of interference and experimental evaluation of resulting part quality,” *Prog Addit Manuf*, vol. 8, no. 4, pp. 759–768, Aug. 2023, doi: 10.1007/s40964-023-00471-2.

[18] “Standard Test Methods for Tension Testing of Metallic Materials.” Mar. 05, 2024. Accessed: Jun. 21, 2024. [Online]. Available: https://compass.astm.org